



OPEN

# Radioactive status of seawater in the northwest Pacific more than one year after the Fukushima nuclear accident

SUBJECT AREAS:  
GEOCHEMISTRY  
ENVIRONMENTAL MONITORING

Wu Men, Jianhua He, Fenfen Wang, Yu Wen, Yiliang Li, Jiang Huang &amp; Xingguang Yu

Laboratory of Marine Isotopic Technology and Environmental Risk Assessment, Third Institute of Oceanography, State Oceanic Administration, 184 Daxue Road, Xiamen 361005, China.

Received  
2 September 2014Accepted  
11 December 2014Published  
13 January 2015Correspondence and  
requests for materials  
should be addressed to  
W.M. (men\_wu@126.  
com)

To understand the impact of Fukushima Nuclear Accident (FNA), eight cruises were performed from 2011–2014. This paper reports the seawater monitoring results of the third cruise, which was conducted in May–June 2012. The northwest Pacific was clearly influenced even more than one year after FNA. However, compared to the monitoring results of the first and second cruises, which were performed in 2011, the seawater radioactivity of the third cruise decreased greatly. The highest value and the highest average of  $^{137}\text{Cs}$  and  $^{134}\text{Cs}$  were found in the 200 m layer, which suggested that  $^{137}\text{Cs}$  and  $^{134}\text{Cs}$  were most likely transported to a depth of 200 m or deeper. At  $21.50^\circ\text{N}$ ,  $125.00^\circ\text{E}$ ,  $^{134}\text{Cs}$  was found at a depth of 200 m, which is 430 km away from the southernmost point of Taiwan Island. The formation and subduction of Subtropical Mode Water is the most reasonable explanation for this process. The coastal water of China was not impacted by the radioactive pollutants released from the FNA. The radiation increments from  $^{137}\text{Cs}$ ,  $^{134}\text{Cs}$  and  $^{90}\text{Sr}$  are only one-thousandth to one-millionth of the screening rate ( $10\ \mu\text{Gy/h}$ ) according to the estimation using ERICA tools.

A major earthquake followed by a tsunami occurred in Japan on 11 March 2011. This event led to the greatest nuclear accident since the Chernobyl disaster in the Fukushima Daiichi nuclear power plant, which negatively influenced the nearby marine environment. A huge amount of radioactive pollutants was released into the northwest Pacific. The accident at the Chernobyl nuclear power plant (NPP) in 1986 demonstrated transparently that radioactive pollutants from a nuclear accident can spread from region to region and across the world, resulting in major damage and long-term environmental effects<sup>1–3</sup>. Although the ocean has a great capacity to dilute and disperse radioactive materials due to its large volume and complex current systems, the long half-lives of radionuclides allow them to remain in marine environments for a long period of time, potentially affecting the environment or human beings via biological concentration and transfer through the marine food chain. Therefore, understanding the fate, transport, and ecological consequences of the long-lived radionuclides in the oceanic environment is of paramount importance. To understand the transport of radioactive pollutants released from the FNA in the northwest Pacific and their potential impact, eight monitoring cruises were conducted by the State Oceanic Administration of China from 2011–2014 (one cruise every half year).

$^{134}\text{Cs}$ ,  $^{137}\text{Cs}$  and  $^{90}\text{Sr}$  are the most important artificial radionuclides released from the FNA. Before the FNA,  $^{137}\text{Cs}$  and  $^{90}\text{Sr}$  could be detected in the ocean, whereas  $^{134}\text{Cs}$  could not be detected. Therefore, if  $^{134}\text{Cs}$  is detected and  $^{137}\text{Cs}$  and  $^{90}\text{Sr}$  exceed their range of background, there is strong evidence of pollutants released from the FNA. This paper reports the monitoring results of  $^{134}\text{Cs}$ ,  $^{137}\text{Cs}$  and  $^{90}\text{Sr}$  of the third cruise, which was performed in May–June 2012. It was very expensive and difficult to perform the monitoring work. There were seldom large-scale monitoring of the radioactive status in the northwest Pacific more than one year after the FNA. Thus, all the data in this paper are important and provide an opportunity to evaluate the radioactive impact of the nuclear accident.

## Methods

**Sampling stations.** Water samples were collected during May–June 2012. The sampling stations are shown in Fig. 1. Black dots signify vertical sampling stations, and blue dots signify surface stations.

**Sampling method.** At vertical stations, samples were collected at depths of 1 m, 100 m and 200 m. For the samples collected at depths of 1 m and 100 m, 125 l of seawater was collected by submersible pumps. For the samples collected at a depth of 200 m, 60 l of seawater was collected

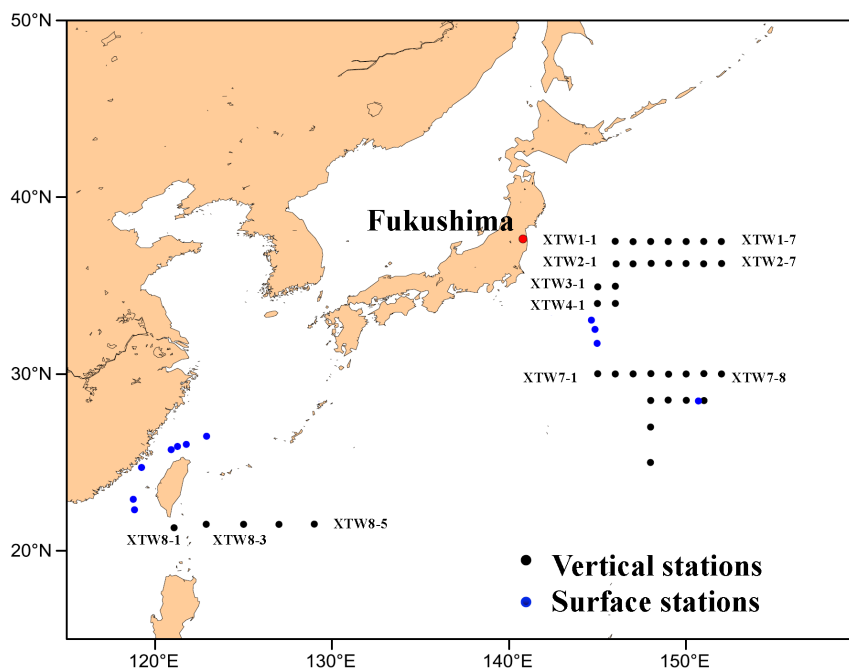


**Figure 1** | Map of sampling stations. This figure was drawn using Surfer.

by a CTD-rosette assembly with Niskin bottle samplers (Model Sea-Bird 911 plus, Sea bird electronics, Inc., Bellevue, Washington, USA.). At the surface stations, only surface seawater was sampled. All of the seawater was stored in polyethylene barrels with acidification.

**Radionuclide measurements.**  $^{134}\text{Cs}$  and  $^{137}\text{Cs}$  were measured using an AMP (ammonium phosphomolybdate) coprecipitation- $\gamma$  spectrometry method according to the Technical Specification for Marine Radioactivity Monitoring issued by the Division of Marine Environmental Protection, State Oceanic Administration of China. (No. 10 [2011] Haihuanzi). Briefly, 30 mg of CsCl and 18 g of AMP were added to 60 l of seawater, and the mixture was stirred and adjusted to obtain a  $\text{pH} \leq 3$ . The mixture was stirred for 30 min until it was well mixed. After standing for more than 24 h, the supernatants were removed by siphoning, and the residual was filtered. After elution 3 times using deionized water, the filter membrane was placed into the muffle and incandesced at  $450^\circ\text{C}$  for 2 h. The residue was measured using a HpGe  $\gamma$  spectrometer to determine the activities of  $^{134}\text{Cs}$  and  $^{137}\text{Cs}$ .

$^{90}\text{Sr}$  was measured by a di (2-ethylhexyl) phosphoric acid (HDEHP) extraction- $\beta$  counting method according to the Technical Specification for Marine Radioactivity Monitoring issued by the Division of Marine Environmental Protection, State Oceanic Administration of China. (No. 10 [2011] Haihuanzi). A total of 2.00 ml of 100 mg/ml  $\text{Sr}(\text{NO}_3)_2$ , 1.00 ml of 20 mg/ml  $\text{Y}(\text{NO}_3)_3$ , 60 g of  $\text{NH}_4\text{Cl}$  and 400 g of  $\text{Na}_2\text{CO}_3$  was added to 40 l of seawater while stirring. The mixture was stirred for 30 min until well mixed. After standing for more than 24 h, the supernatants were removed by siphoning, and the residual was filtered. A total of 300–400 ml of 10 mol/l  $\text{HNO}_3$  was used to dissolve the sediment. The solution was extracted twice using 50 ml of 10% di (2-ethylhexyl) phosphoric acid (HDEHP), and the organic phase was re-extracted twice using 20 ml of 10 mol/l  $\text{HNO}_3$ . A total of 5 ml of  $\text{C}_2\text{H}_2\text{O}_4$  was added to form a saturated solution, and the solution was adjusted to  $\text{pH} = 1.5\text{--}2.0$  using a 6 mol/l  $\text{NH}_3\text{H}_2\text{O}$  solution and 2 mol/l  $\text{HNO}_3$ . Finally, the  $\text{YC}_2\text{O}_4$  sediment was produced. The  $\text{YC}_2\text{O}_4$  was filtered and placed into  $\alpha/\beta$  counter to determine the activity of  $^{90}\text{Y}$ . The activity of  $^{90}\text{Sr}$  was then calculated from the  $^{90}\text{Y}$  data according to a special formula.

For the samples collected at a depth of 200 m, only 60 l of seawater was obtained. The collected seawater was used for the measurement of  $^{134}\text{Cs}$  and  $^{137}\text{Cs}$ , but there was not enough sample to measure  $^{90}\text{Sr}$ .

## Results

**Concentrations of  $^{134}\text{Cs}$ ,  $^{137}\text{Cs}$  and  $^{90}\text{Sr}$ .** The contents of  $^{134}\text{Cs}$ ,  $^{137}\text{Cs}$  and  $^{90}\text{Sr}$  are shown in Tab. 1. The activities of  $^{134}\text{Cs}$  ranged from undetected to  $9.68 \text{ Bq/m}^3$ , with an average of  $1.21 \text{ Bq/m}^3$ . The activities of  $^{137}\text{Cs}$  ranged from 0.41 to  $18.10 \text{ Bq/m}^3$ , with an average of  $3.39 \text{ Bq/m}^3$ . The activities of  $^{90}\text{Sr}$  ranged from 0.56 to  $3.57 \text{ Bq/m}^3$ , with an average of  $1.49 \text{ Bq/m}^3$ . The background data before the FNA are also listed in Tab. 1. According to the data from IAEA's MARiS database from 2000 to 2010, the radioactivity of  $^{137}\text{Cs}$  in surface seawater near Japan ranged from 0.04 to  $3.4 \text{ Bq/m}^3$ , with

an average of  $1.7 \pm 0.6 \text{ Bq/m}^3$  ( $n = 961$ ).  $^{134}\text{Cs}$  was usually not detectable in surface seawater because there has been no new major source over the past 20 years and the  $^{134}\text{Cs}$  that has been released over the last century has decayed to an extremely low level, which is below the detection limit. The activity of  $^{90}\text{Sr}$  in surface seawater in the northwest Pacific was 0.01 to  $2.6 \text{ Bq/m}^3$ , with an average  $1.2 \pm 0.4 \text{ Bq/m}^3$  ( $n = 871$ ). The monitoring data in this report were clearly higher than the monitoring data from before the FNA.

**Distributions of  $^{134}\text{Cs}$  and  $^{137}\text{Cs}$ .** The distributions of  $^{134}\text{Cs}$  and  $^{137}\text{Cs}$  at depths of 1 m, 100 m and 200 m are shown in Fig. 2 and Fig. 3, respectively. A total of 52% of the surface sample contained  $^{134}\text{Cs}$ . However, that amount increased to 70% and 69% at the 100 m layer and 200 m layer, respectively. Generally speaking,  $^{134}\text{Cs}$  was found as far south as  $21^\circ\text{N}$  (200 m) and as far east as  $152^\circ\text{E}$ .  $^{137}\text{Cs}$  was found at all sample stations. From the surface to a depth of 200 m, the activities of  $^{137}\text{Cs}$  and  $^{134}\text{Cs}$  increased with increasing depth. At a

Table 1   Concentrations of $^{134}\text{Cs}$ , $^{137}\text{Cs}$ and $^{90}\text{Sr}$		Activities ( $\text{Bq/m}^3$ )		
Depths	Statistical items	$^{137}\text{Cs}$	$^{134}\text{Cs}$	$^{90}\text{Sr}$
1 m	min	0.91	nd	0.56
	max	4.78	2.70	3.57
	average	2.14	0.43	1.38
100 m	min	0.41	nd	0.95
	max	8.97	4.76	2.94
	average	3.39	1.26	1.60
200 m	min	0.55	nd	/
	max	18.10	9.68	/
	average	5.49	2.41	/
All layers	min	0.41	nd	0.56
	max	18.10	9.68	3.57
	average	3.39	1.21	1.49
Coastal Background (2000–2010)*		0.04–3.40	nd	0.01–2.60
		$1.7 \pm 0.6$ ( $n = 961$ )	/	$1.2 \pm 0.4$ ( $n = 871$ )

nd means not detected.

\*from IAEA's MARiS Database.

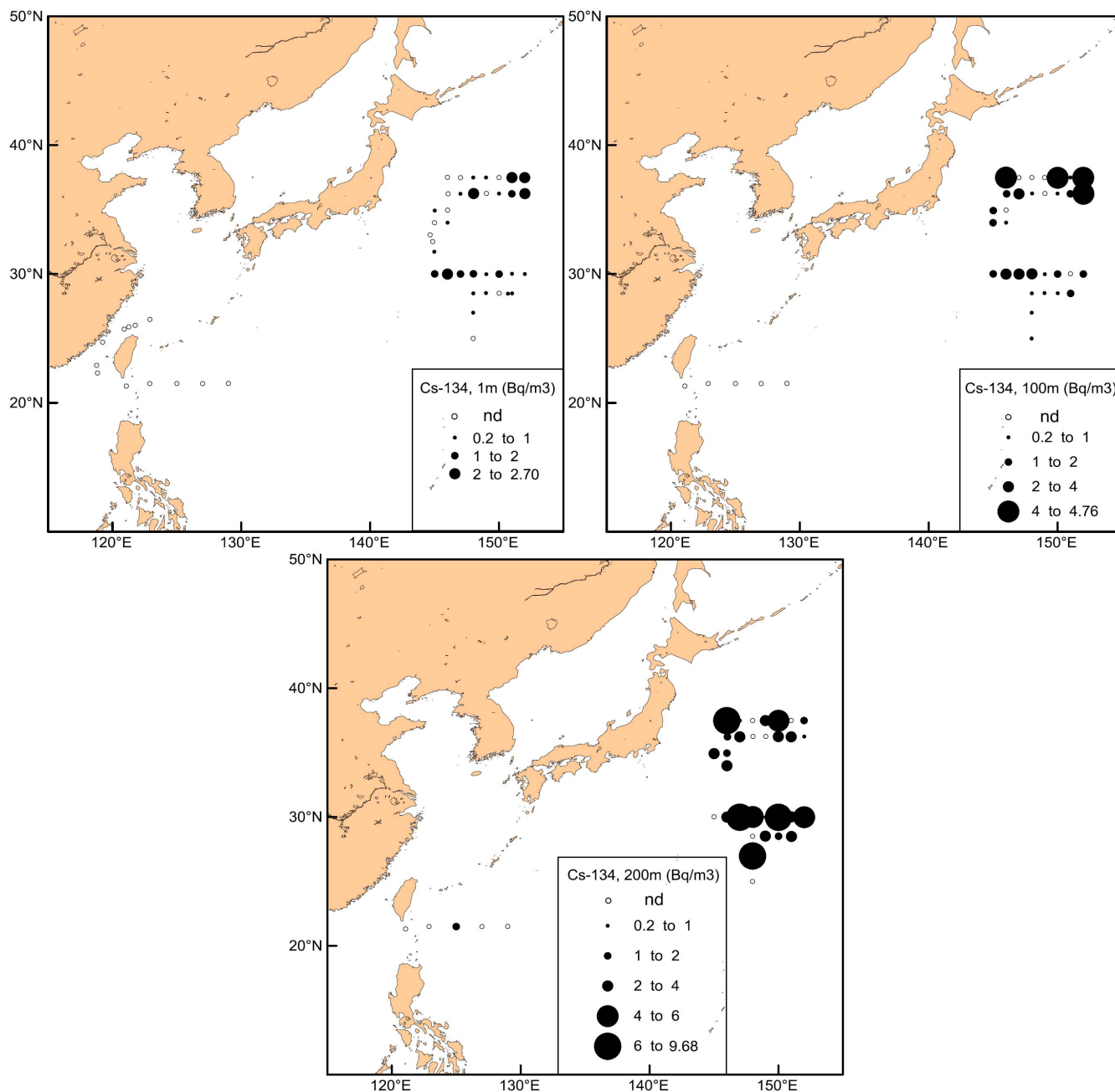


**Figure 2** | The distributions of  $^{134}\text{Cs}$  at depths of 1 m, 100 m and 200 m in the North Pacific. These figures were drawn using Surfer.

depth of 200 m, both  $^{137}\text{Cs}$  and  $^{134}\text{Cs}$  had the highest values. At the adjacent sea area of Taiwan Island,  $^{134}\text{Cs}$  was not found in the surface water and 100 m layer. However, at a depth of 200 m,  $^{134}\text{Cs}$  was found ( $1.99 \pm 0.23 \text{ Bq/m}^3$ ) at  $21.50^\circ\text{N}$ ,  $125.00^\circ\text{E}$ , which is 430 km away from the southernmost point of Taiwan Island.

**The distributions of  $^{90}\text{Sr}$ .** The distributions of  $^{90}\text{Sr}$  at depths of 1 m and 100 m are shown in Fig. 4.  $^{90}\text{Sr}$  was found in all samples. Unlike  $^{137}\text{Cs}$  and  $^{134}\text{Cs}$ ,  $^{90}\text{Sr}$  activities did not clearly change with depth and instead were relatively uniform. The highest  $^{90}\text{Sr}$  activity was only slightly higher than the upper limit of the background (Tab. 1).

## Discussion

**Variation in radioactivity level.** The highest activities and the average activities of the three artificial radionuclides from June 2011 to June 2012 are shown in Fig. 5. The first monitoring cruise was conducted in June 2011. The highest activities of  $^{137}\text{Cs}$ ,  $^{134}\text{Cs}$  and

$^{90}\text{Sr}$  were approximately 400 ~ 800 km away from Fukushima, reaching up to  $800 \text{ Bq/m}^3$ . However, the activities of the three nuclides decreased with each subsequent cruise. The second monitoring cruise was conducted in December 2011. The highest activities of  $^{137}\text{Cs}$  and  $^{134}\text{Cs}$  decreased ten-fold to approximately  $80 \text{ Bq/m}^3$ . In the third cruise, the activities decreased even further. Comparing the monitoring data to the previous radioactivity data before the FNA, we can conclude that the northwest Pacific was clearly influenced by the accident even after one year had passed.

**Transport of artificial radionuclides.** Marine scientists want to know how radioactive pollutants are transported in the North Pacific Ocean, and many numerical simulations have been reported<sup>4-7</sup>. The radioactive pollutants from the FNA were transported eastward at a speed of approximately 200 km/month<sup>8</sup>, which was consistent with the trajectories of Argo floats launched near the Fukushima nuclear power plant. The pollutants are thus

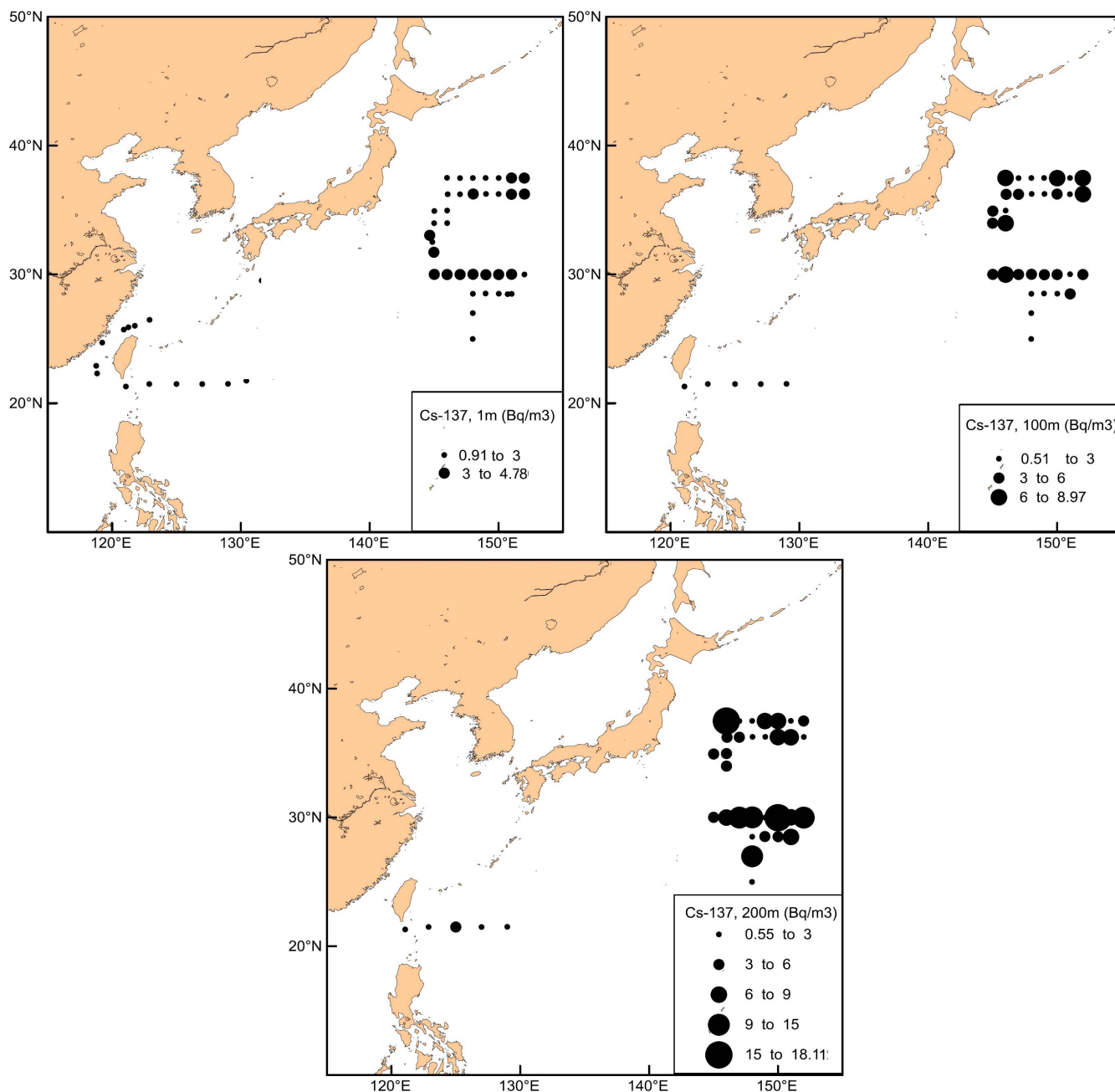


**Figure 3** | The distributions of  $^{137}\text{Cs}$  at depths of 1 m, 100 m and 200 m in the North Pacific. These figures were drawn using Surfer.

expected to reach the coastal water of the USA after approximately 4–6 years following the North Pacific Current (Fig. 6)<sup>5,7,9</sup>. The entire North Pacific Ocean will be labeled with Fukushima  $^{137}\text{Cs}$  10 years after the accident<sup>7</sup>. Mesoscale eddies are expected to disperse radioactivity in complicated patterns. The radioactivity of  $^{137}\text{Cs}$  was rapidly diluted and dispersed in the North Pacific Ocean<sup>5</sup>. The mesoscale eddies in the Kuroshio Extension played an important role in diluting radioactive cesium<sup>4</sup>, which is why  $^{134}\text{Cs}$  was found as far east as  $152^\circ\text{E}$  and had relatively low activities more than one year after the accident. Because there were no other stations in the area east of  $152^\circ\text{E}$ , we were unable to determine how far east the radioactive pollutants were transported.

The highest value and the highest average of  $^{137}\text{Cs}$  and  $^{134}\text{Cs}$  were found in the 200 m layer. Kumamoto et al. (2014) determined that radioactive pollutants can penetrate to depths of 200 m through surface cooling and vertical mixing in the winter, which supports our results. We were unable to determine how deep the radioactive

pollutants were transported because we did not take samples from water deeper than 200 m. However, according to Kumamoto et al. (2014)<sup>8</sup>,  $^{134}\text{Cs}$  penetrated to a depth of approximately 300 m between  $35^\circ\text{N}$  and  $40^\circ\text{N}$  along the  $149^\circ\text{E}$  meridian Jan–Feb 2012. Therefore, in May–June 2012, the radioactive pollutants were probably transported to the deeper area than 300 m.

At  $21.50^\circ\text{N}$ ,  $125.00^\circ\text{E}$ , the station XTW8-3,  $^{134}\text{Cs}$  was found at a depth of 200 m, which is 430 km away from the southernmost point of Taiwan Island. The presence of  $^{134}\text{Cs}$  in this location is unusual. It was unusual that the radioactive pollutants were transported from  $37^\circ\text{N}$  to  $21.5^\circ\text{N}$  so quickly just over one year after the accident. It was also unusual that  $^{134}\text{Cs}$  was not detected at the surface and 100 m depth but only at a depth of 200 m. Finally, it remains to be explained why  $^{134}\text{Cs}$  was not detected at other stations except for the one at  $21.50^\circ\text{N}$ ,  $125.00^\circ\text{E}$ . We re-checked the data and verified that they are accurate. After excluding the possibility that the data was incorrect, we determined that there was a possible explanation for the unusual

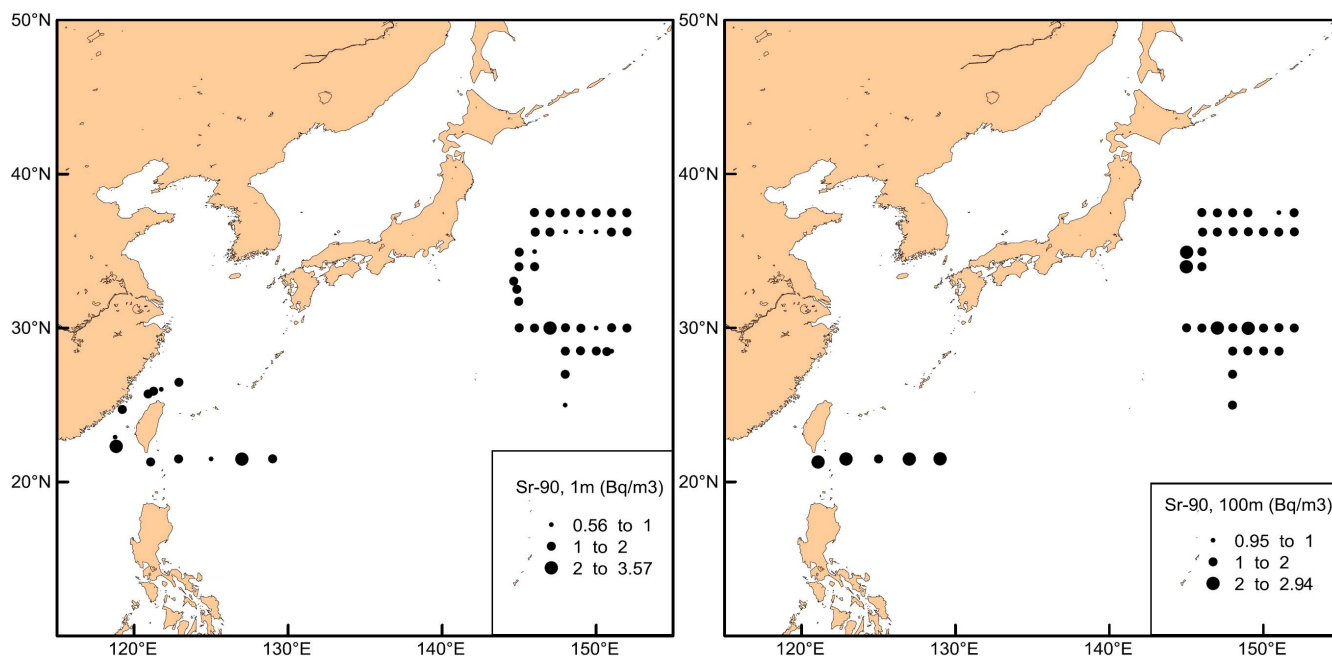


**Figure 4** | The distributions of  $^{90}\text{Sr}$  at depths of 1 m and 100 m in the North Pacific. These figures were drawn using Surfer.

findings. This was that the detected  $^{134}\text{Cs}$  was derived from the formation and subduction of Subtropical Mode Water (STMW)<sup>8</sup>. To the south of the Kuroshio Extension (KE) between 30°N and 35°N, STMW is formed and penetrates to a depth of approximately 400 m ( $25.6 \delta_\theta$ ) in late winter. This STMW then spreads to the nearly subtropical front through advection over the Kuroshio recirculation region<sup>9–10</sup> (Fig. 6).  $^{134}\text{Cs}$  in the North Pacific Ocean occurred mainly in March 2011, when STMW was just being formed. Therefore, the  $^{134}\text{Cs}$  that arrived to the south of the KE was most likely immediately mixed vertically to depths of 300–400 m. The  $^{134}\text{Cs}$  in newly formed STMW then started to spread to approximately 20°N along subsurface isopycnals ( $25.0\text{--}25.6 \delta_\theta$ )<sup>8</sup>. According to relevant STMW references<sup>11–17</sup>, the essential features of STMW are that the potential vorticity no greater than  $2.0 \times 10^{-10}/\text{m}\cdot\text{s}$ , the depth is 150 ~ 350 m, the salinity is 34.6 ~ 34.8, the temperature is 16 ~ 18°C, and the potential density is  $25.0\text{--}25.6 \delta_\theta$ . The potential vorticity was calculated using the following equation:  $PV = (f/\rho) (\Delta\delta_\theta/\Delta Z)$ <sup>10</sup>, where  $f$  is the Coriolis parameter,  $\rho$  is the density of seawater,  $\Delta\delta_\theta$  is the difference between adjacent potential vorticity layers and  $\Delta Z$  is the interval between adjacent potential vorticity layers. For a depth of 200 m at station XTW8-3, the potential vorticity was  $2.0 \times 10^{-10}/\text{m}\cdot\text{s}$ ,

the potential density was  $25.13 \delta_\theta$ , the salinity was 34.72, and the temperature was 17.73°C (Tab. 2). These values agreed well with the essential features of STMW. The time required for  $^{134}\text{Cs}$  emitted from the Fukushima nuclear power plant to enter the formation area of STMW is approximately 1 ~ 2 months<sup>8</sup>. From there, approximately one year is needed to transport the radioactive material via STMW from the area of formation (35°N) to low-latitude areas near 23°N<sup>10</sup>. The speed required is 1°/month (12° over 12 months). Based on this speed, we calculated that  $^{134}\text{Cs}$  released from the Fukushima nuclear power plant and transported to 21.5°N requires approximately 14.5 ~ 15.5 months. In this report,  $^{134}\text{Cs}$  that was released during the FNA was transported to 21.5°N 15 months after the accident. The predicted time scale is consistent with the actual situation. Based on an analysis of our own data regarding potential vorticity, depth, salinity, temperature, potential density and time scale, we have demonstrated that only the seawater at a depth of 200 m at 21.50°N and 125.00°E was most likely from the STMW at station XTW8-3. Contour maps of temperature, salinity and potential density for section XTW8 at depths of 0–500 m are shown in Fig. 7. The essential features of STMW in section XTW8 are marked by the different colors. By overlapping

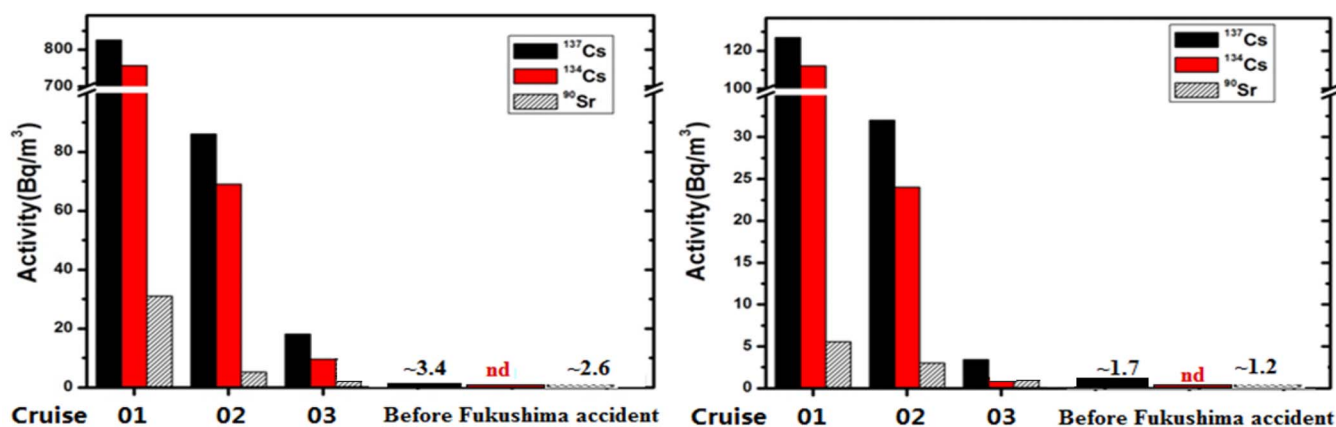


**Figure 5** | Variations in the highest activities (left) and the average activities (right) in the North Pacific during cruises 1–3. This figure was drawn using Origin.

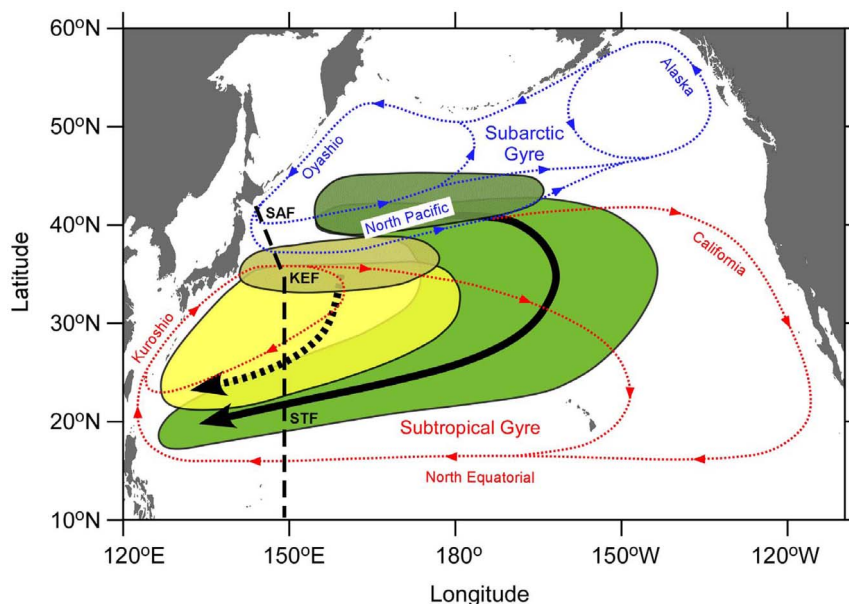


**Figure 6** | A schematic view of the formation and subduction of mode waters in the North Pacific. The yellow and yellow-shaded ellipses indicate spreading and formation areas, respectively, of STMW ( $25.0\text{--}25.6 \delta_\theta$ ). The green and green-shaded areas indicate spreading and formation areas, respectively, of Central Mode Water (CMW) ( $26.0\text{--}26.6 \delta_\theta$ ), which is denser than STMW. The thick broken and solid arrows show the spreading directions of STMW and CMW, respectively. The blue and red dotted lines are surface water currents of the subarctic and subtropical gyres, respectively. SAF, KEF, and STF indicate the subarctic, Kuroshio Extension, and subtropical fronts along the observational line, respectively. This figure was cited from the literature<sup>9</sup>.

the three maps, it is clear that the STMW exists between depths of 200 m and 300 m; however, observations were only collected at a depth of 200 m in this area (Fig. 7). As shown in Tab. 2, the calculated potential densities at a depth of 200 m for the other stations in section XTW8 are out of the range of typical STMW values (i.e.,  $25.0\text{--}25.6 \delta_\theta$ ). Therefore, only the seawater sample from a depth of 200 m at station XTW8-3 was from STMW. This is a possible reason for why  $^{134}\text{Cs}$  was not detected at the surface and a depth of 100 m at station XTW8-3.

**Radioactive levels in the coastal water of China.** There were 9 stations in the northeast of the South China Sea. A comparison of the monitoring data of these stations with the background data reveals that  $^{137}\text{Cs}$  and  $^{90}\text{Sr}$  were within the range of the background data and  $^{134}\text{Cs}$  could not be detected, which suggests that the coastal water of China has not been impacted by the radioactive pollutants released from the FNA.

**Radiological risk assessment.** In recent decades, the importance of radiation assessment for non-human species has been recognized<sup>18</sup>. There are various radiation assessment tools, of which the ERICA tool is the best. ERICA (Environmental Risk from Ionising Contaminants: Assessment and Management) provides an integrated approach to the scientific, managerial and societal issues surrounding the environmental effects of contaminants emitting ionizing radiation, with an emphasis on biota and ecosystems<sup>19</sup>. The ERICA Assessment Tool (June 2011 version) was used to evaluate radiological risk in the marine environment of the monitoring area. The Tier 2 assessment was completed. Isotopes of  $^{137}\text{Cs}$ ,  $^{134}\text{Cs}$ ,  $^{90}\text{Sr}$  and a dose screening value of  $10 \mu\text{Gy/h}$  were selected in the assessment. The highest activity concentrations of  $^{137}\text{Cs}$ ,  $^{134}\text{Cs}$  and  $^{90}\text{Sr}$  in the seawater monitoring results were input into the assessment. The environmental concentration, parameters of distribution coefficient (Kd), concentration ratio (CR), dose conversion coefficients of radiation, occupancy factors, and an

**Table 2** | The temperature, salinity, potential density, potential vorticity of section XTW8

Station	Longitude ( $^{\circ}\text{E}$ )	Latitude ( $^{\circ}\text{N}$ )	Depth (m)	Temperature ( $^{\circ}\text{C}$ )	Salinity	Potential density ( $\delta_\theta$ )	Potential vorticity ( $\times 10^{-10}/\text{m}\cdot\text{s}$ )
XTW8-1	121.07	21.5	3	29.30	33.54	20.87	2.0
			100	27.47	34.30	22.05	6.4
			200	19.88	34.54	24.45	7.7
XTW8-2	122.89	21.5	6	29.06	34.01	21.30	0.1
			100	26.22	34.53	22.62	6.8
			200	20.46	34.85	24.54	3.4
XTW8-3	125.00	21.5	1	28.71	34.15	21.53	10.7
			100	20.50	34.85	24.52	8.3
			200	17.73	34.72	25.13	2.0
XTW8-4	127.00	21.5	8	27.76	34.51	22.11	0.1
			100	21.77	34.87	24.19	2.5
			200	18.45	34.77	24.99	2.4
XTW8-5	128.99	21.5	1	27.95	34.63	22.14	14.7
			100	21.61	34.84	24.21	4.4
			200	18.98	34.79	24.87	1.7

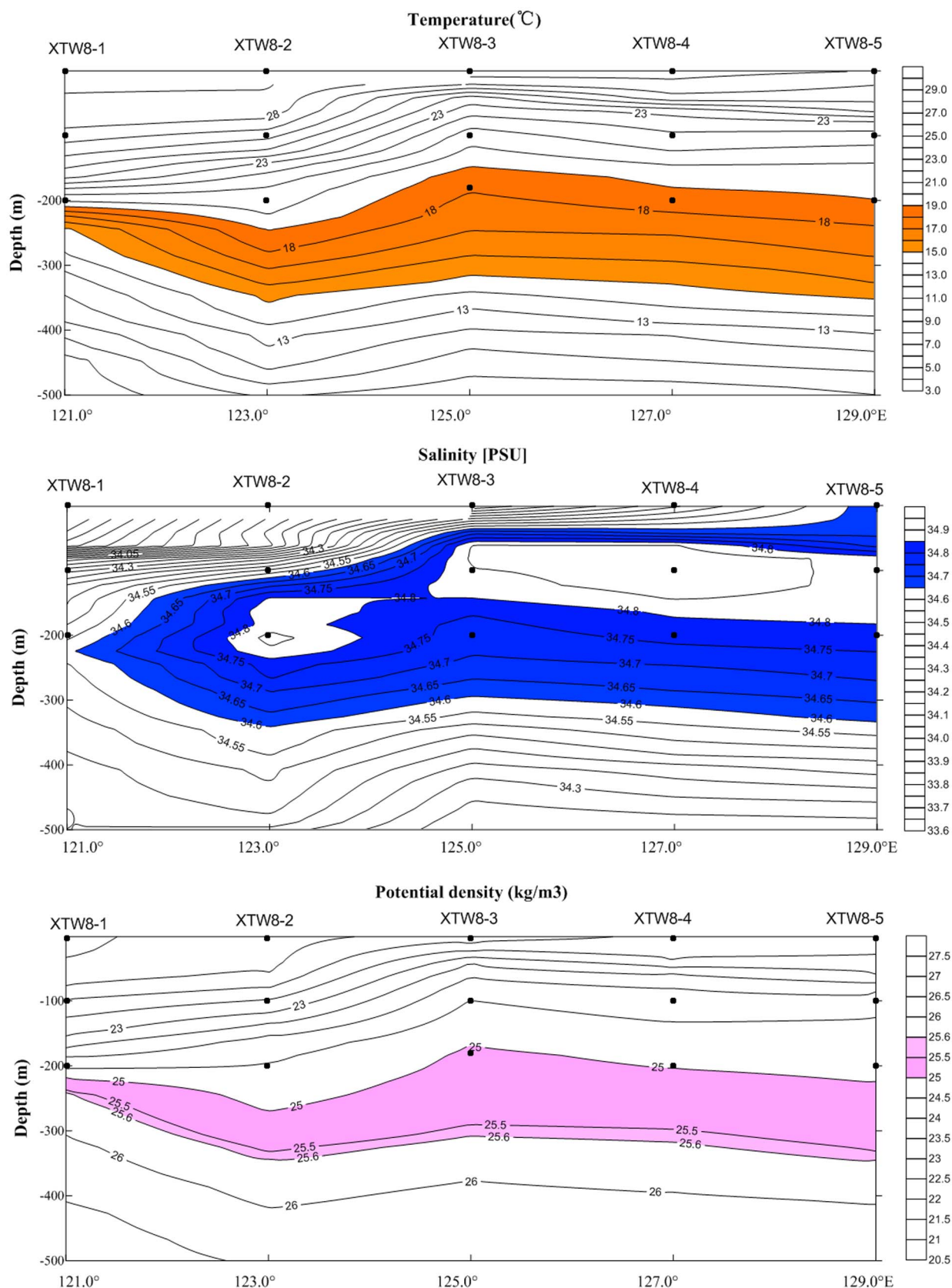


**Figure 7** | Maps of temperature, salinity and potential density of the section XTW8. These figures were drawn using Surfer.

uncertainty factor were all set as the default value in the ERICA Tool. The weighting factors of low beta, beta/gamma and alpha were set to 3, 1 and 20, respectively. The output results of the Tier 2 assessment are listed in Tab. 3, where all of the total dose rates per organism were

lower than the screening rate by approximately 3–6 orders of magnitude. These findings suggest that the radiation increments that come from the  $^{137}\text{Cs}$ ,  $^{134}\text{Cs}$  and  $^{90}\text{Sr}$  released from the FNA are only one-thousandth to one-millionth of the screening rate (10  $\mu\text{Gy/h}$ ).



Table 3 | Total dose rate results in the ERICA tool Tier 2 assessment

Biota	External Dose Rate [ $\mu\text{Gy}/\text{h}$ ]			Internal Dose Rate [ $\mu\text{Gy}/\text{h}$ ]			Total Dose Rate [ $\mu\text{Gy}/\text{h}$ ]			Total Dose Rate [ $\mu\text{Gy}/\text{h}$ ] per organism
	Cs-134	Cs-137	Sr-90	Cs-134	Cs-137	Sr-90	Cs-134	Cs-137	Sr-90	
Pelagic fish (Wading) birds	7.45E-06	5.07E-06	7.14E-08	9.80E-04	1.58E-03	3.24E-06	9.87E-04	1.59E-03	3.31E-06	2.58E-03
Benthic fish	1.59E-02	1.09E-02	8.03E-07	1.42E-04	2.65E-04	4.93E-05	1.60E-02	1.11E-02	5.01E-05	2.72E-02
Benthic mollusks	1.68E-02	1.16E-02	1.24E-06	7.67E-05	1.79E-04	2.48E-04	1.69E-02	1.18E-02	2.50E-04	2.89E-02
Crustaceans	1.53E-02	1.05E-02	3.69E-07	7.94E-05	1.34E-04	2.92E-05	1.54E-02	1.06E-02	2.96E-05	2.60E-02
Macroalgae	1.74E-02	1.23E-02	3.21E-06	1.10E-04	2.82E-04	6.75E-05	1.75E-02	1.26E-02	7.07E-05	3.02E-02
Mammals	3.87E-06	2.53E-06	1.50E-08	1.20E-03	1.25E-03	3.34E-06	1.20E-03	1.26E-03	3.36E-06	2.46E-03
Phytoplankton	7.84E-06	5.25E-06	9.64E-08	1.58E-04	2.80E-04	5.09E-05	1.66E-04	2.85E-04	5.10E-05	5.02E-04
Polychaete worms	9.58E-06	8.51E-06	2.32E-06	4.24E-09	1.03E-08	5.70E-09	9.59E-06	8.52E-06	2.33E-06	2.04E-05
Reptiles	3.41E-02	2.39E-02	3.14E-06	1.92E-04	4.56E-04	9.06E-07	3.43E-02	2.43E-02	4.05E-06	5.86E-02
Sea anemones or true corals - colony	3.97E-06	2.72E-06	1.64E-08	2.58E-03	2.66E-03	3.34E-06	2.59E-03	2.67E-03	3.36E-06	5.26E-03
Sea anemones or true corals - polyp	1.51E-02	1.01E-02	1.09E-06	7.72E-04	1.24E-03	2.07E-03	1.59E-02	1.14E-02	2.07E-03	2.93E-02
Vascular plants	1.72E-02	1.19E-02	2.41E-06	3.68E-04	9.63E-04	1.79E-03	1.76E-02	1.29E-02	1.79E-03	3.23E-02
Zooplankton	1.68E-02	1.16E-02	1.11E-06	2.77E-05	5.97E-05	8.70E-05	1.69E-02	1.16E-02	8.81E-05	2.86E-02
	8.81E-06	6.34E-06	1.29E-06	8.94E-05	2.39E-04	4.76E-06	9.83E-05	2.45E-04	6.05E-06	3.50E-04

## Conclusions

The activities of the artificial radionuclides  $^{137}\text{Cs}$ ,  $^{134}\text{Cs}$  and  $^{90}\text{Sr}$  in the seawater of the northwest Pacific decreased with time. In May–June 2012, on the third monitoring cruise of the west Pacific,  $^{134}\text{Cs}$  was found in 63.7% of the samples. A total of 32.9% of the  $^{137}\text{Cs}$  data were higher than the highest value measured before the FNA ( $3.4 \text{ Bq}/\text{m}^3$ ). The west Pacific was clearly affected by the accident even though more than one year had passed.

$^{134}\text{Cs}$  was found as far south as  $21^\circ\text{N}$  (200 m) and as far east as  $152^\circ\text{E}$ . From the surface water to the deep water, the activities of  $^{137}\text{Cs}$  and  $^{134}\text{Cs}$  increased with increasing depth. At a depth of 200 m, both  $^{137}\text{Cs}$  and  $^{134}\text{Cs}$  had the highest values. At  $21.50^\circ\text{N}$ ,  $125.00^\circ\text{E}$ ,  $^{134}\text{Cs}$  was found at a depth of 200 m, which is 430 km away from the southernmost point of Taiwan Island. The formation and subduction of Subtropical Mode Water (STMW) seems a reasonable explanation for this unusual situation. The formation and subduction of Subtropical Mode Water (STMW) seems a reasonable explanation for this unusual situation. The STMW is formed and penetrates to a depth of approximately 400 m ( $25.6 \delta_\theta$ ) south of the KE between  $30^\circ\text{N}$  and  $35^\circ\text{N}$  in late winter before spreading to the nearly subtropical front through advection over the Kuroshio recirculation region. The radioactive pollutants are brought to the deep water (300–400 m) and transported to approximately  $20^\circ\text{N}$  along subsurface isopycnals ( $25.0$ – $25.6 \delta_\theta$ ). Based on an analysis of our own data regarding potential vorticity, depth, salinity, temperature, potential density and time scale, we have demonstrated that only the seawater at a depth of 200 m at  $21.50^\circ\text{N}$  and  $125.00^\circ\text{E}$  is most likely from the STMW, which successfully explains why  $^{134}\text{Cs}$  was not detected at the surface and a depth of 100 m depth at station XTW8-3.

A comparison of the monitoring data with the background data reveals that the coastal water of China has not been impacted by the radioactive pollutants released from the FNA.

The radiation increments from the  $^{137}\text{Cs}$ ,  $^{134}\text{Cs}$  and  $^{90}\text{Sr}$  released from the FNA are only one-thousandth to one-millionth of the screening rate ( $10 \mu\text{Gy}/\text{h}$ ).

All the data reported could be used as actual measured data to correct the parameters of interest for numerically modeling the radionuclide transport in the northwest Pacific.

- Balonov, M. I. The Chernobyl Forum: major findings and recommendations. *J. Environ. Radioactiv.* **96**, 6–12 (2007).
- Pollanen, R., Valkama, I. & Toivonen, H. Transport of radioactive particles from the Chernobyl accident. *Atmos. Environ.* **31**, 3575–3590 (1997).
- Saenko, V. *et al.* The Chernobyl accident and its consequences. *Clin. Oncol.* **23**, 234–243 (2011).
- Kawamura, H., Kobayashi, T., Furuno, A., Usui, N. & Kamachi, M. Numerical simulation on the long-term variation of radioactive cesium concentration in the North Pacific due to the Fukushima disaster. *J. Environ. Radioactiv.* **136**, 64–75 (2014).
- Behrens, E., Schwarzkopf, F., Lübbecke, J. & Böning, C. W. Model simulations on the long-term dispersal of  $^{137}\text{Cs}$  released into the Pacific Ocean off Fukushima. *Environ. Res. Lett.* **7**, 1–10 (2012).
- Maderich, V. *et al.* Regional long-term model of radioactivity dispersion and fate in the Northwestern Pacific and adjacent seas: application to the Fukushima Dai-ichi accident. *J. Environ. Radioactiv.* **131**, 4–18 (2014).
- Nakano, M. & Povinec, P. P. Long-term simulations of the  $^{137}\text{Cs}$  dispersion from the Fukushima accident in the world ocean. *J. Environ. Radioactiv.* **111**, 109–115 (2012).
- Kumamoto, Y. *et al.* Southward spreading of the Fukushima-derived radiocesium across the Kuroshio Extension in the North Pacific. *Sci. Rep.* **4**, 4276 (2014).
- Suga, T. & Hanawa, K. The mixed layer climatology in the northwestern part of the North Pacific subtropical gyre and the formation area of Subtropical Mode Water. *J. Mar. Res.* **48**, 543–566 (1990).
- Suga, T. & Hanawa, K. The subtropical mode water circulation in the North Pacific. *J. Phys. Oceanogr.* **25**, 958–970 (1995).
- Hanawa, K. & Yoritaka, H. North Pacific subtropical mode water observed in long XBT cross sections along  $32.5^\circ\text{N}$  line. *J. Oceanogr.* **57**, 679–692 (2001).
- Suga, T., Takei, Y. & Hanawa, K. The mixed layer climatology in the north Pacific subtropical gyre: the central mode water and the subtropical mode water. *J. Phys. Oceanogr.* **27**, 140–142 (1996).
- Suga, T., Hanawa, K. & Toba, Y. Subtropical mode water in the  $137^\circ\text{E}$  section. *J. Oceanogr.* **19**, 1605–1618 (1989).





14. Song, X. Z., Lin, X. P., Padmore, M. R., Zheng, P. N. & Qian, H. Spacial structure and annual variation estimated from Argo float data for subtropical mode water in the Northwest Pacific Ocean(in Chinese). *Adv. Mar. Sci.* **27**, 1–10 (2009).
15. Pan, A. J. *Subtropical mode water and its formation mechanism in the north pacific(in Chinese)*. Doctor thesis, Ocean University of China, Qingdao, 2004.
16. Aoyama, M., Uematsu, M., Tsumune, D. & Hamajima, Y. Surface pathway of radioactive plume of TEPCO Fukushima NPP1 released  $^{134}\text{Cs}$  and  $^{137}\text{Cs}$ . *Biogeosciences*. **10**, 3067–3078 (2013).
17. Talley, L. D. Potential vorticity distribution in the north pacific. *J. Phys. Oceanogr.* **18**, 89–106 (1988).
18. Valentin, J. A Framework for assessing the impact of ionising radiation on non-human species. *Ann ICRP*. **33**, 66–207 (2003).
19. Larsson, C. M. An overview of the ERICA Integrated Approach to the assessment and management of environmental risks from ionising contaminants. *J. Environ. Radioactiv.* **99**, 1364–1370 (2008).

## Acknowledgments

This work is supported by a fund from Ecological Environment Protection Division, State Oceanic Administration (SOA), People's Republic of China and by the Scientific Research Foundation of Third Institute of Oceanography. SOA. NO.TIOSOA2011.

## Author contributions

W.M. performed the data analysis and wrote the paper. J.H., W.M. and X.Y. performed the cruise. W.M., J.H., F.W., W.Y. and Y.L. performed the radionuclide measurements in the lab. J.H. provided the data of the physical oceanography. All authors reviewed the manuscript.

## Additional information

**Competing financial interests:** The authors declare no competing financial interests.

**How to cite this article:** Men, W. *et al.* Radioactive status of seawater in the northwest Pacific more than one year after the Fukushima nuclear accident. *Sci. Rep.* **5**, 7757; DOI:10.1038/srep07757 (2015).



This work is licensed under a Creative Commons Attribution-NonCommercial-NoDerivs 4.0 International License. The images or other third party material in this article are included in the article's Creative Commons license, unless indicated otherwise in the credit line; if the material is not included under the Creative Commons license, users will need to obtain permission from the license holder in order to reproduce the material. To view a copy of this license, visit <http://creativecommons.org/licenses/by-nc-nd/4.0/>